heritage

Article

Pluvial Flood Risk Assessment in Urban Areas: A Case Study for the Archaeological Site of the Roman Agora, Athens

Theano Iliopoulou *, Panayiotis Dimitriadis and Demetris Koutsoyiannis

Department of Water Resources, School of Civil Engineering, National Technical University of Athens, Heroon Polytechneiou 5, GR-157 80 Zografou, Greece; pandim@itia.ntua.gr (P.D.); dk@itia.ntua.gr (D.K.)
* Correspondence: tiliopoulou@hydro.ntua.gr

Abstract: Ancient monuments located in urbanized areas are subject to numerous short- and long-term environmental hazards with flooding being among the most critical ones. Flood hazards in the complex urban environment are subject to large spatial and temporal variability and, thus, require location-specific risk assessment and mitigation. We devise a methodological scheme for assessing flood hazard in urban areas, at the monument's scale, by directly routing rainfall events over a fine-resolution digital terrain model at the region of interest. This is achieved using an open-source 2D hydraulic modelling software under unsteady flow conditions, employing a scheme known as 'direct rainfall modelling' or 'rain-on-grid'. The method allows for the realistic representation of buildings and, thus, is appropriate for detailed storm-induced (pluvial) flood modelling in urbanized regions, within which a major stream is usually not present and conventional hydrological methodologies do not apply. As a case study, we perform a pilot assessment of the flood hazard in the Roman Agora, a major archaeological site of Greece located in the center of Athens. The scheme is incorporated within an intelligent decision-support system for the protection of monumental structures (ARCHYTAS), allowing for a fast and informative assessment of the flood risk within the monument's region for different scenarios that account for rainfall's return period and duration as well as uncertainty in antecedent wetness conditions.

Keywords: risk assessment; storm events; flood risk; pluvial flooding; urban areas; monuments; cultural heritage; direct rainfall modelling; rain-on-grid; uncertainty

Citation: Iliopoulou, T.; Dimitriadis, P.; Koutsoyiannis, D. Pluvial Flood Risk Assessment in Urban Areas: A Case Study for the Archaeological Site of the Roman Agora, Athens. *Heritage* **2023**, *6*, 7230–7243. https://doi.org/10.3390/heritage6110379

Academic Editors: Humberto Varum, Fernanda Prestileo and Vasilis Sarhosis

Received: 17 October 2023
Revised: 15 November 2023
Accepted: 16 November 2023
Published: 20 November 2023

1. Introduction

Ancient monuments are exposed to a multitude of environmental conditions and natural hazards that are often the cause of their degradation or even destruction. The identification and mitigation of environmental risks faced by monuments has been of increasing interest in recent decades, in the frame of cultural heritage protection [1–9].

The environmental risks can be divided into two categories: (a) the slowly evolving risks arising from the cumulative exposure of the monument to normal environmental conditions and causing gradual deterioration of the construction material and degradation of the aesthetic value of the monument, and (b) the rapidly evolving risks from earthquakes and extreme weather phenomena, which directly threaten the monument itself as well as the site visitors. The first category pertains to a multitude of atmospheric, climatic, and environmental conditions that cumulatively, over the span of time, cause physico-chemical changes in the construction material, a phenomenon widely known as weathering (e.g., [10,11]). The second category of risks includes flood risk, risks from extreme rainfall, including landslides and erosion, risks from extreme wind loads, fire risks, as well as seismic risks. In monuments located in urban environments, aside from the seismic risk, the most relevant risk associated with natural hazards is considered to be that of flooding at the archaeological site [4,6,12–14].

Unlike other risks of structural nature, flood risks have a strong local character, depending on topographic features changing even on a small scale, causing high spatiotemporal variability and uncertainty [15]. Thus, areas that may be just a few meters apart can have significant differences in flood depth and velocity, as both the proximity and elevational position in relation to the hydrographic network play an important role. This spatial uncertainty is magnified in the urban regions, where the built environment, including buildings and roads as well as smaller-scale obstacles such as parked cars, exerts major controls on the flow direction [16]. At the same time, the imperviousness of the urban surface leads to a higher volume of flow compared to the natural system. The particularly complex urban topography is the main difference between floods in an urban area and floods in a natural environment, as well as the main reason for the increasing complexity of the phenomenon.

The dominant approach in the urban flood literature is that the discharge, derived from previous rainfall-runoff analysis, acts as the key design quantity and input to hydrodynamic models (e.g., [16–18]). However, often, in many urbanized regions, major surface watercourses are not present and, therefore, the conventional methodology of hydrograph routing in riverside areas may not be applicable. In addition, the complex geometry and topography of the urban environment have a decisive effect on the passage of the flood, as not only the flow velocity but also the direction of the flow of water in the urban environment is affected by the existence of artificial structures such as buildings and roads [17]. In this respect, urban hydrodynamic models are quite sensitive to the reduction of spatial resolution, mainly due to the homogenization of the topographical complexity of the urban environment. The latter leads to the underestimation of the volume available for water storage as well as to the inaccurate simulation of small-scale routing processes which are greatly affected by the various obstructions to the flow [19]. Although different approaches exist to address this issue (e.g., the porosity concept, [19]), less is known about the case in which one needs a detailed flood risk assessment of an urban region in the absence of a major stream. This would also be the case for an urban region of high cultural interest, such as a site of cultural heritage and a monumental construction.

To address this issue, we formulate a methodology that directly routes design rainfall events over a fine resolution digital terrain model, while accounting for the at-site variability in the soil infiltration capacity. To produce 2D flood inundation maps without involving hydrograph routing, we employ a state-of-the-art methodological scheme of 2D hydraulic models that allows the direct routing of rainfall events over an elevation grid, known as 'direct rainfall' or 'rain-on-grid' [20]. The scheme is integrated in the ARCHYTAS platform, an archetypal telemetry and decision support system for the protection of monumental structures [21]. The platform is developed within the frame of the ARCHYTAS project (http://archytas.ntua.gr/, accessed on 15 November 2023) with the aim to assist the Agencies of the Ministry of Culture and relevant authorities of the Greek state to prioritize inspection, maintenance, and rehabilitation actions before or after hazardous events at sites of cultural heritage. It stores a database of results for synthetic rainfall events enabling a fast and informative assessment of the flood risk in the monument's region for various synthetic scenarios of rainfall's return period, event duration, and antecedent wetness conditions.

2. Study Area

The flood risk is estimated for the wider area of the Roman Agora, a 0.011 km^2 archaeological site at the center of Athens, where the monument of the Horologion of Andronikos Cyrrhestes (also known as Tower of the Winds) is located (Figure 1). The monument was constructed in the first half of the 1st century B.C. by the astronomer Andronicos, from Kyrrhos, Macedonia and is considered the first meteorological station in history. On the upper part of each side, the winds are depicted using their symbols and their names are engraved. Outside there were sundials, while inside there was a hydraulic clock. The area of the monument was chosen not only for the symbolism but also because of its geographical location which constitutes a topographic depression making it vulnerable to flooding.

(**a**)

(**b**)

Figure 1. (**a**) Satellite photo of the Roman Agora area from Google Maps; (**b**) Southeast view of the Tower of the Winds (Horologion of Andronikos Cyrrhestes).

The Agora, in its most flood-prone topographical region, i.e., on its south and southeast side, is surrounded by walls that prevent the intrusion of floodwaters from higher altitudes. Therefore, it can be approached as a closed hydrological sub-basin. However, it is noted that the north and northwest sides are not protected by walls and, in the event of a major flood in the wider area and failure of the urban drainage network, it is possible that part of the floodwaters from the adjacent road surfaces may be received.

Ancient Greek and Roman water drainage systems existed at the Agora but have been disturbed and are only partially functional after the conservation [22]. Nowadays, the drainage system consists of two small culverts (diameter ~0.2 m) located at the lower topographic area (the lower terrain of the Agora where the Peristyle is located) and an underground drainage network also on the lower terrain of the Agora constructed to address the rise of the underground water table—an issue that has been reported in the past [22,23]. A small percentage of impermeable surfaces exists within the area and include the entrance areas and corridors of the courtyards as well the area of buildings, namely the monument of interest, the entrance gate, the Fethiye Mosque, storage areas, etc. From the latter, the major buildings that are accounted for herein are the Fethiye Mosque, a rectangular-sized ottoman church within the area, and the monument of interest, an octagonal marble tower, as shown in Figure 1b.

3. Methods

A special feature of the monument area is that it is located within the urban fabric, in a sub-basin without open-surface watercourses; as such, the methodology developed differs from the conventional approach to flood hazard assessment in riverside areas. Instead, a methodology is developed for direct routing of stormwaters in the two-dimensional space, consisting of a suite of hydrological models and a 2D hydraulic model as described next.

3.1. Rainfall Modelling

The first step of hydrological modelling pertains to the estimation of the rainfall depth for a given return period and timescale of interest based on local historical data. This is obtained through the design rainfall (also called ombrian) curves at the basin, i.e., the relationship linking intensity (x), reference time scale (k), and return period (T) of rainfall. For the area of the Roman Agora, the regional rainfall curves of Attica were used, which vary according to the altitude of the study area [24]. For the study area located at an altitude lower than 160 m, the relationship yielding the rainfall intensity for any return period and time scale of minutes to a few days is the following:

$$x = 445 \frac{(T/0.07)^{0.07} - 1}{(1 + k/0.1)^{0.73}} \quad (1)$$

where x is the rainfall intensity in mm/h, k is the time scale in hours (h), and T is the return period in years. The values resulting from Equation (1) refer to the intensity of point rainfall, instead of surface average intensities which are typically applied for watershed analyses. However, for a small region such as the study area, equal to 0.011 km^2, the surface reduction is negligible [25].

Subsequently, a method is required for the temporal disaggregation of the rainfall depth for a given duration of a rainfall event, i.e., the design hyetograph. One of the most realistic disaggregation methods for design practices [26] is the alternating block (AB) method ([27], pp. 31–35; [28], p. 466). The total rainfall depth is partitioned into sectional depths (blocks) arranged in time sequence with a desired resolution, with the maximum in the middle of the selected total duration and the rest in descending order alternating left and right of the central block. The cumulative rainfall depth at each time step is estimated using Equation (1) and then the partial depths are derived.

The above procedure yields a design rainfall event for a given duration and return period. However, it is the infiltration capacity of the soil that controls the amount of rainfall that is actually transformed into surface runoff, i.e., the so-called active (excess) rainfall. To calculate the infiltration losses and separate them from the total hyetograph, the US Soil Conservation Service method is applied [29]. The method is based on the following assumptions:

- For an initial interval t_{a_0}, the entire rainfall amount h_{a_0} corresponding to this interval is completely converted into a deficit (initial deficit), giving no excess rainfall at all. Consequently, after time t_{a_0}, the maximum effective rain depth cannot exceed the potential quantity $h - h_{a_0}$, where h is the total rainfall depth during the event.
- The additional deficit, beyond the initial h_{a_0}, during a heavy rainfall cannot exceed a maximum value S, which is called potential maximum retention. The initial deficit is $h_{a_0} = 0.2\,S$.
- At each time $t > t_{a_0}$, the ratios of the excess rainfall depth and the deficit minus the initial deficit ($h_a - h_{a_0}$), to the corresponding potential quantities ($h - h_{a_0}$ and S, respectively), are equal. Based on the above assumptions, the following empirical relationship for the estimation of the excess rainfall is derived:

$$h_e = \begin{cases} 0 & h \le 0.2S \\ \frac{(h - 0.2S)^2}{h + 0.8S} & h > 0.2S \end{cases} \quad (2)$$

Equation (2) is applied both for the final rainfall depth and for its block values and, thus, the temporal evolution of the event is obtained. The final depth of the deficits can asymptotically reach (for major rainfall events) the value 1.2 S.

In the case that there are no runoff measurements, the value of the parameter S can be estimated from the literature. Specifically, the value of S (in mm) is linked to another characteristic parameter of the basin, which is known as the runoff curve number (CN), through the following relationship:

$$S = 254\left(\frac{100}{\mathrm{CN}} - 1\right) \tag{3}$$

The CN parameter takes values from 0 to 100 and is determined from the soil conditions and land uses in the watershed, as well as from the antecedent soil moisture (wetness) conditions.

To describe the uncertainty about the value of the CN parameter, the parameter is treated as a random variable that follows a uniform distribution in the range [60, 90]. From this range, three representative scenarios are studied, i.e., CN = 65, 75, and 85. The first corresponds to a high soil infiltration capacity, the second to intermediate, and the last to a lower capacity. The range selection was based on the literature for this type of land use and cover in the study area, i.e., open space with >50% grass cover, considering soil with spatially moderate infiltration capacity [30]. The spatial infiltration capacity is higher in the open space area of the southern inner Peristyle due to the existence of an underground drainage network on the floor of the Agora [22,23] but is reduced in the area of the monument in the access areas/corridors of the courtyards and in the area of buildings located within the study area (entrance gate, Fethiye Mosque, storage area, etc.).

Therefore, the value CN = 75 was considered representative of the spatially average infiltration capacity of the area. The highest and lowest values of CN represent the range of uncertainty of the parameter due to its bibliographic determination but are also characteristic of the temporal variation in soil moisture conditions throughout the year. In particular, the value CN = 65 for a soil type with given infiltration properties, represents a low soil-moisture content and, therefore, a higher infiltration capacity, indicative of a dry season (e.g., after a prolonged absence of rainfall). Correspondingly, for the same soil type, the CN = 85 value represents high soil moisture content (and, thus, lower infiltration capacity) due to a wet (rainy) season and/or a rise in the underground water table in the region [22,23].

Based on the above assumptions, the excess rainfall hyetographs are derived for a given value of the duration and return period of the rainfall event and for the three values of the CN parameter (65, 75, and 85). Due to the small size of the study area, the studied durations of the design rainfall events were equal to 1 h and 2 h. The excess rainfall hyetographs are the input data of the hydraulic model described next.

3.2. Hydraulic Model: Direct Rainfall Modelling

The assessment of the flood risk consists of the calculation of various output parameters of the flood inflow, such as the maximum flow depth, the maximum flow velocity, or the time evolution and duration of these during a storm and flood event. Due to the relatively flat topography (i.e., small average flood plain slope) in the study area, the developed flow velocities are expected to be generally small, while the monitoring of the temporal evolution of the flood event for rainfall durations of 1 h and 2 h may be considered of little importance given the small area of interest. Thus, the maximum depth of flow that can occur at each point of the study area during a rainfall event is selected as the most critical flood risk assessment output parameter, and the inflow (through the design rainfall depth and curve number), roughness, and floodplain slope are considered as the most important input parameters (a methodology for selecting the input and output parameters related to their uncertainty during a flood event can be seen through benchmark experiments in [15]).

Two-dimensional hydrodynamic models represent flood flow as a two-dimensional field assuming that the third dimension, flow depth, is small relative to the other two. Therefore, for the estimation of the two-dimensional average flow velocity in the cross-section, the solution of the Saint-Venant unsteady flow equations in the two-dimensional field, i.e., the Navier–Stokes equations adapted for shallow water (also known as shallow-water equations), is needed. The open-source hydraulic software HEC-RAS 6.0 (Hydrologic Engineering Center CEIWR-HEC River Analysis System, [31]) developed by the US Army Corps of Engineers is used to estimate the flow parameters in the area. From the available models of the software, the scheme of two-dimensional hydraulic calculations in unsteady flow conditions is applied using a spatially uniform design hyetograph (as obtained from the previous step), as an external boundary condition. The software then performs runoff routing due to uniformly distributed rain in the ground topography solving the two-dimensional Saint-Venant equations (in the diffusion or dynamic Eulerian-Lagrangian scheme), i.e., applying the 'direct rainfall method'. The latter is a modern hydraulic method, the effectiveness of which depends primarily on the high resolution of the digital elevation model combined with that of the computational grid, where the former is suggested to be less than 1 m [20].

For this purpose, a very detailed digital terrain model (DTM) with a resolution of 0.2 m was produced for the wider area of the Roman Agora, in which, in addition to the ground elevations, the elevation surfaces of the most important buildings within the study area are depicted, that is the monument of interest (Tower of the Winds) and the Fethiye Mosque, as shown in Figure 2. The computational mesh was developed as a two-dimensional grid, which has an area equal to the watershed and a spatial resolution for most of the region equal to 0.5 m. For reasons of model stability in areas of steep slope changes due to above-ground constructions, a coarser grid resolution of approximately 2 m was chosen in the areas of the buildings (refinement regions tool; Figure 2). The simulation was carried out using a time step of 1 s in order to satisfy the Courant et al. [32] condition for the given cell size (0.5–2 m), while the duration of the simulation was chosen in order for the maximum flow depth to occur.

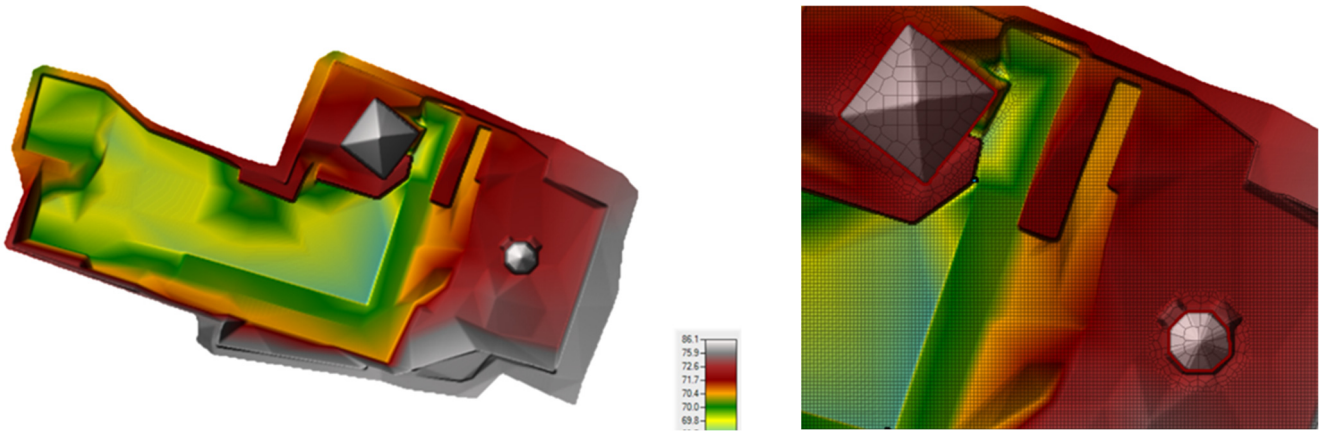

(**a**) (**b**)

Figure 2. (**a**) Digital terrain model of the monument's area also representing the major buildings. (**b**) Zoom in the computational grid in the area of the buildings.

The locations of the two culverts (internal diameter ~0.2 m) identified during a field-investigation in the area, i.e., of the main culvert located at the lowest topographical point at the floor of the Agora and another culvert in the area of the Peristyle near the Mosque, were also included in the model as external boundary conditions. The Manning roughness coefficient, which also plays an important role in the estimated maximum depth, is selected to be uniform for the whole area and equal to n = 0.06, according to the international literature for the given land cover type and similar analyses [18,33].

For the unsteady flow analysis, the excess hyetograph for a given duration, return period, and CN parameter, applied uniformly over the 2D mesh and the output hydrographs at the locations of the two culverts, are used as boundary conditions. For an internal diameter of 0.2 m, the maximum discharge capacity of each culvert was estimated as 0.05 m^3/s. For each rainfall event, the corresponding output hydrographs were estimated through iterative approximations of the model so that the final volumetric error was less than 5% and the outflow followed the temporal evolution of the inflow at the locations of the culverts with a minimum value of 0 and a maximum possible value equal to their discharge capacity. For rainfall durations of 1 h and 2 h, it was found that simulation durations of 2 h and 3 h, respectively, were sufficient to observe the maximum flow depth at each point of the area.

From the simulation, the maps of maximum flow depth corresponding to a synthetic rainfall event of specific duration (D), return period (T), and soil infiltration capacity (CN) emerged. The simulations are run for six different return periods from T = 5 years up to T = 1000 years, for CN = 65, 75, and 85 and durations of D = 1 h and 2 h. For each of these scenarios, the corresponding maximum flow depth flood maps are produced.

3.3. Scenario Database and ARCHYTAS Platform

The general properties of the monument (geographic location, Google Earth background, name, etc.) are entered into the management subsystem of the ARCHYTAS platform. There, the coordinates of the monument are defined (latitude and longitude) and any necessary images are imported. Google Earth is used as a background for the visualization of flood risk.

The flood-risk assessment process based on the methodology developed in the previous sections is quite time-consuming, due to the computational time of the hydraulic simulation (of the order of 20 min for an average scenario); therefore, it is not possible to perform the simulation 'on the fly' on the platform. For this purpose, it is necessary to create a database of results for all combinations of the parameters with values of D = 1 and 2 h, return periods T = 5, 10, 50, 100, 500, and 1000 years, and infiltration capacities CN = 65, 75, and 85. These amount to 36 combinations.

The original result files are .tiff files produced using the HEC-RAS software. To allow processing of these files and customize the visualization of the results, the .tiff files are imported into the ArcGIS 10 software where the selected visualization is determined, and the final flood depth maps are produced as .png image files. Each of the .png files in the database is named by encoding the characteristics of the design rainfall event to which it corresponds, i.e., the rainfall duration, the return period, and the soil infiltration capacity parameter CN. For example, a file named 'D1T5CN75' corresponds to a 1 h rain scenario, a 5-year return period, and CN = 75. This set of image files corresponding to 'pre-run' scenarios forms the results database of the platform.

Based on a preliminary examination of the area, flood risk is related to the accessibility of the archaeological site and the requirement to remove stagnant water and clean the monument. Therefore, for the assessment of the vulnerability by the user of the platform, it is sufficient to import the satellite image of the monument area through Google Earth as a background for the visualization of the maximum flow depth and its spatial distribution.

4. Results

4.1. Design Rainfall Hyetographs

The 36 flood scenarios correspond to 36 design excess rainfall hyetographs. The different combinations yield different plausible profiles for the excess rainfall both in terms of the total depth and its temporal distribution. For the same return period and soil infiltration capacity, a larger duration corresponds to a higher total rainfall depth that is, in turn, more likely to exceed the soil infiltration capacity and, thus, contribute to increased surface runoff (Figure 3). For the same return period and rainfall duration, increased values of the CN parameter result in a faster onset of the excess rainfall hyetograph and an increase

in its total amount, while the opposite occurs for lower values, as shown in Figure 4. Finally, for the same CN values and rainfall duration, a larger return period of the rainfall depth naturally yields a more severe event.

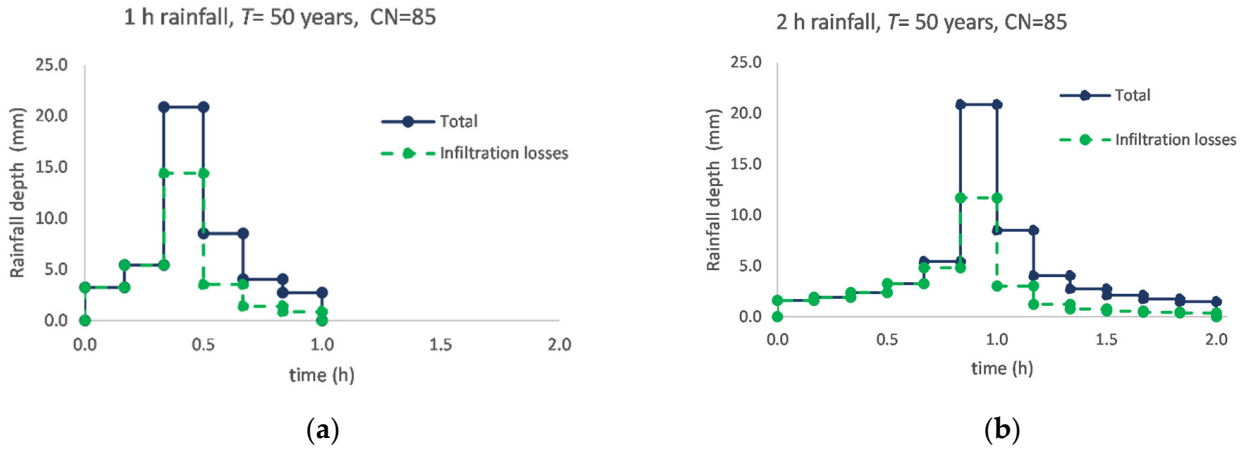

(**a**) (**b**)

Figure 3. Total design rainfall hyetograph based on the AB method for durations of 1 h (**a**) and 2 h (**b**), a 50-year return period, and corresponding infiltration losses (mm) of CN = 85.

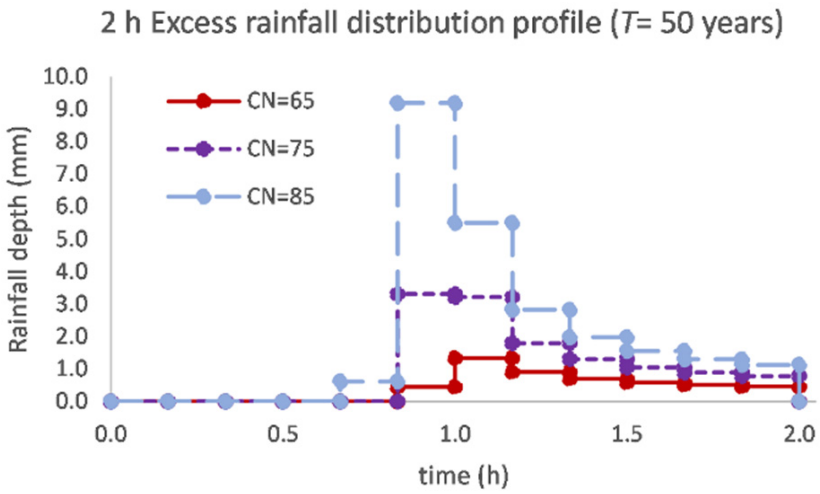

Figure 4. Excess (effective) rainfall hyetographs for a 2 h duration and 50-year return period for three different CN values, 65, 75, and 85.

4.2. Flood Maps

For each of the 36 synthetic rainfall events, the hydraulic model is run according to the procedure outlined in Section 3.2, and a maximum flood depth map is derived. The resulting flood depths are categorized into six classes as seen in Figure 5. A flooding event does not occur for only two scenarios corresponding to durations 1 h and 2 h, respectively, a return period of 5 years, and a high infiltration capacity (CN = 65). In these cases, almost all rainfall amount is lost to infiltration and, therefore, excess rainfall is close to 0; thus, no flooding occurs. In all other cases, some amount of flooding occurs, ranging from negligible for small return periods to more severe for return periods equal or higher to 100 years, as shown in Figure 5.

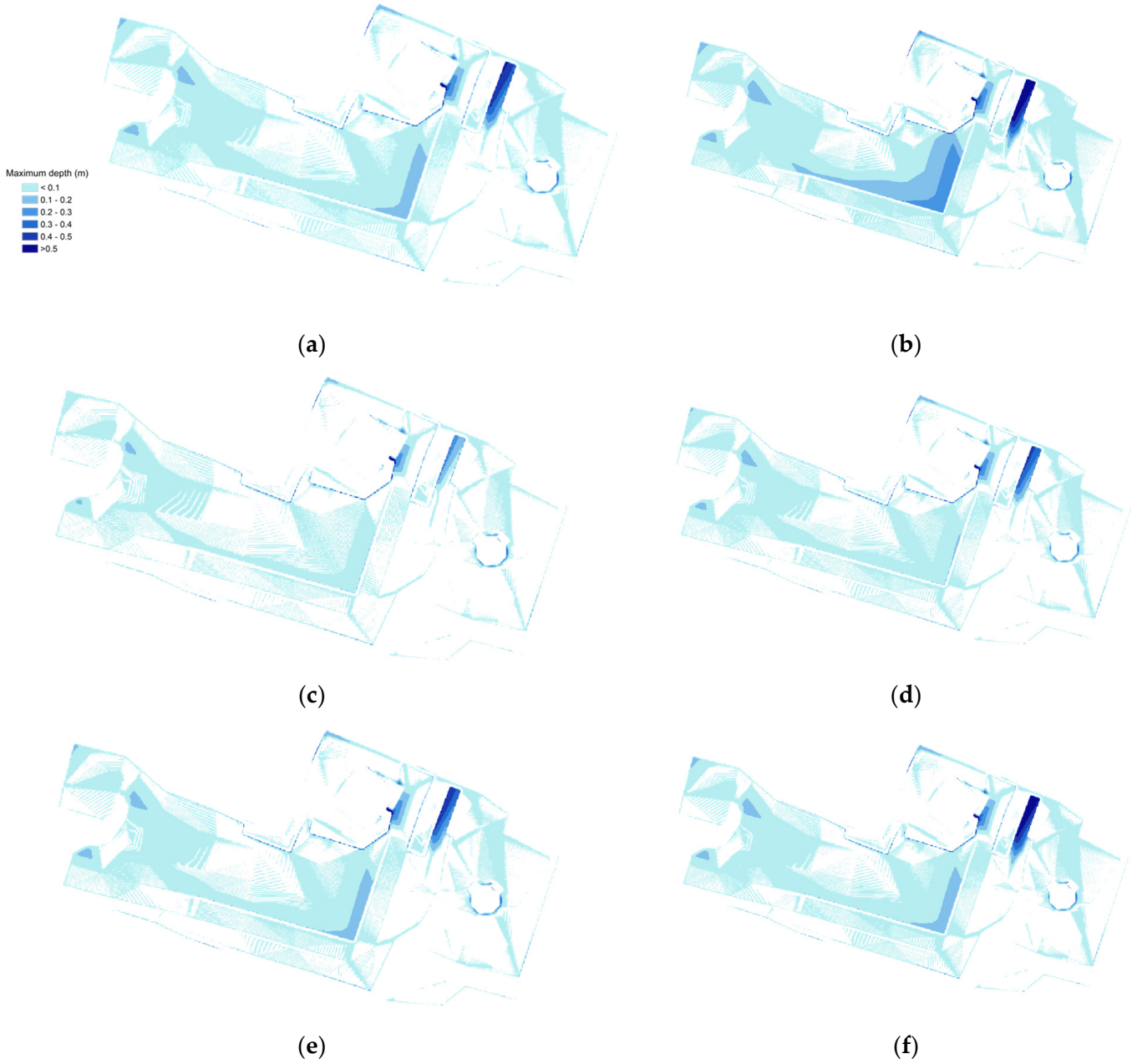

Figure 5. Upper row: maximum flood depths for D = 1 h, CN = 85, and T = 100 years (**a**) or T = 1000 years (**b**). Medium row: maximum flood depths for T = 50 years, D = 1 h, and CN = 75 (**c**) or CN = 85 (**d**). Lower row: maximum flood depths for T = 500 years, CN = 75, and D = 1 h (**e**) or D = 2 h (**f**).

An interesting observation is that the effect of the soil infiltration capacity is large on the results being comparable to, or even larger (in the case of small rainfall durations) than, the effect of the return period of the rainfall depth. For instance, a 1 h 100-year return period event in the condition of high soil moisture content, i.e., low infiltration capacity (CN = 85), yields a slightly higher excess rainfall depth than the same-duration, 500-year rainfall event coupled with a higher infiltration capacity (CN = 75) (cf. Figure 5a,e). This reflects the fact that flooding is a combination of hydrometeorological conditions with the soil infiltration capacity exerting a major control on flood magnitude, aside from the intensity of the rainfall event. This is particularly the case for small event durations, where the total rainfall depth may be well within the limits of the soil infiltration capacity. Consequently, for average wetness conditions and return periods smaller or equal to 50 years, which is the standard

for hydrological design in Greece, flooding is minimal at the area accessible to the visitors (Figure 5c,d), also due to the culverts' operation within their design limits. This is validated using the locals' experience at the site, reporting only a few moderate flooding incidents in the lower terrain area.

More severe flooding is observed for return periods of 100 years and higher coupled with medium or low infiltration capacity, in which cases the culverts' discharge capacity is significantly exceeded (Figure 5a,b,e,f). In these cases, duration, increasing the excess rainfall depths, acts as an aggravating factor, yet this mostly affects the areas not drained by the culverts such as local depression areas (Figure 5e,f). In all studied cases, however, up to 1000-year return periods and even under an adverse soil moisture state, it is affirmed that the monument itself does not face an immediate flood risk which is consistent with the topography of its location, being higher than the largest part of the Agora. On the other hand, the most flood-prone areas of the Agora, as indicated by most simulations, are the lower terrain area (where the main culvert is located) and a local depression area in the northeast region where Roman latrines were located (called 'Vespasianae'). Both these areas were validated as flood-prone during an onsite visit, as seen in Figure 6.

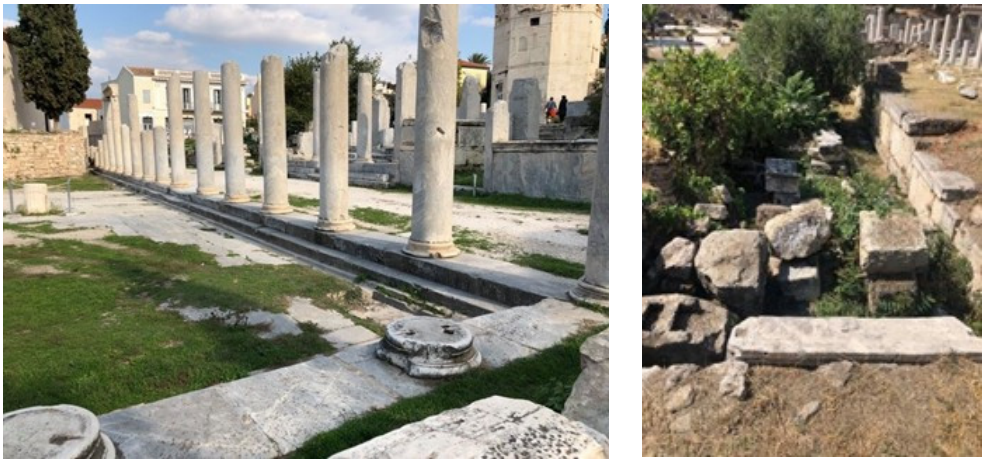

(**a**) (**b**)

Figure 6. View of regions identified as the most vulnerable to flooding at the study area: (**a**) The lower terrain of the Agora (aside the Peristyle); (**b**) The area of the roman latrines.

4.3. Risk Assessment Using the ARCHYTAS Platform

The above flood maps are stored as image files encoded according to the methodology outlined in Section 3.3 so that they correspond to a unique combination of a synthetic rainfall event and a soil infiltration capacity.

Using the generated scenario database, the ARCHYTAS platform yields a corresponding flood map depending on the user's parameter selection, as seen in Figure 7. The user selects the return period, the rainfall duration and an estimate of the soil's infiltration capacity (based on assessment of the soil moisture state) and the resulting flood map is overlayed on the Google map's background of the area. This allows a first examination of areas at risk of widespread flooding as well as an indication of the areas where stagnant waters may be present and, thus, require cleaning (i.e., in the Vespasianae region). A short informational text is also available to aid the user in the selection of these parameters.

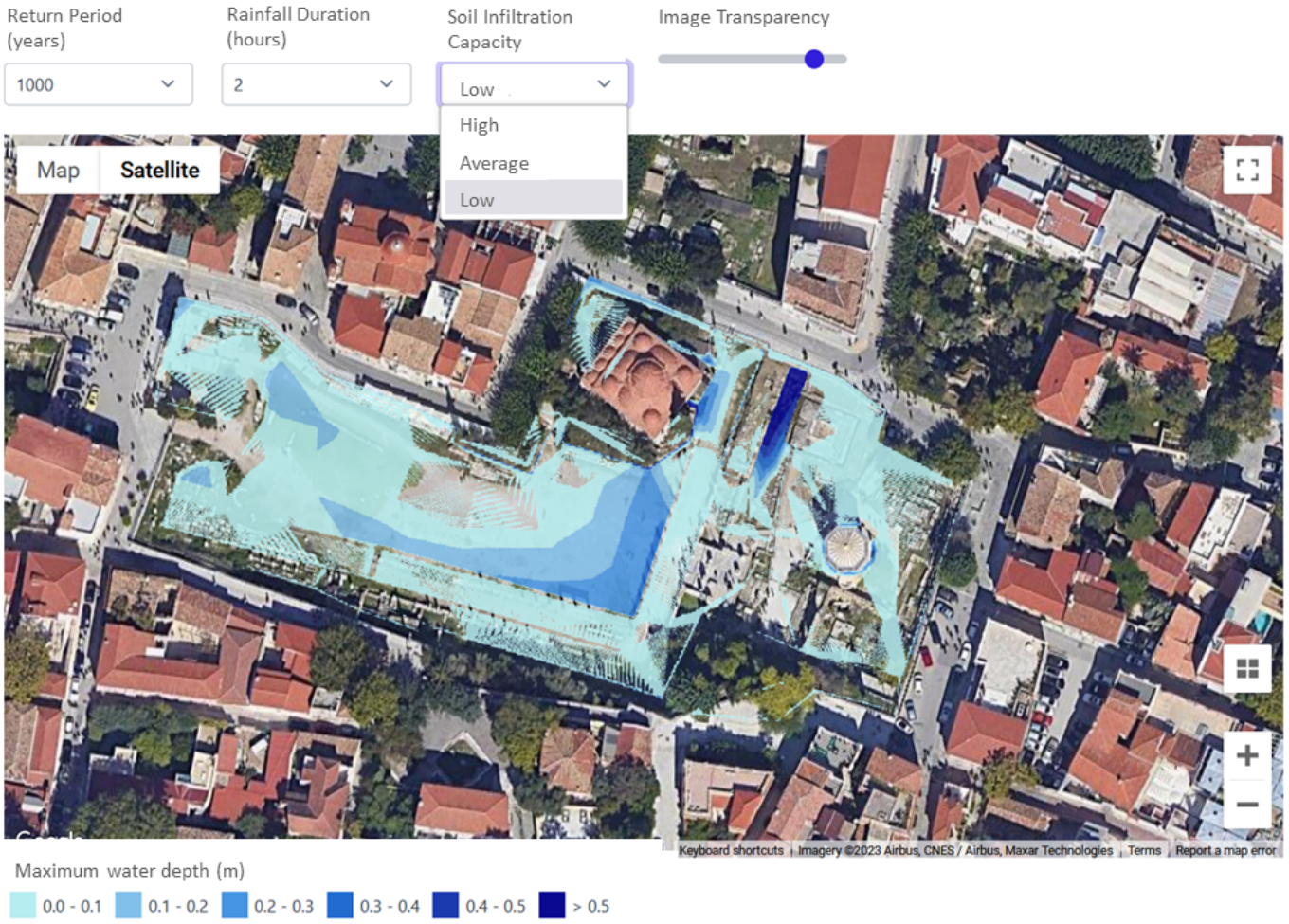

Figure 7. ARCHYTAS user interface for flood risk assessment in the monument's region (Roman Agora).

5. Discussion and Conclusions

Both recent experience and our theoretical understanding of the flood process at the urban scale suggest that flooding should be considered for the safety assessment of ancient monuments. Flood modelling in urban regions, however, is challenging since it integrates a range of uncertainties from the topographical representation of the complex urban environment to the inherent hydrodynamic and hydroclimatic uncertainty. A methodological gap also exists in the case flood risk from extreme rainfall needs to be assessed in an urban area of high interest, such as an archaeological site, in the case where open surface watercourses (e.g., a major stream) are not present and the conventional hydrograph routing methodology is not applicable.

Towards this aim, a new methodology has been applied to assess pluvial flood risk for such an area, i.e., the Roman Agora in Athens, Greece, an archaeological site within the historical center of the city, where the monument of the Tower of the Winds is located. The modelling suite comprises the following: (a) At-site design rainfall (ombrian) curves; (b) An excess rainfall model accounting for infiltration losses and incorporating uncertainty in terms of the spatiotemporal infiltration capacity; (c) A 2D hydraulic model routing the uniformly distributed excess rainfall over the entire region of interest using the unsteady flow equations and the 'direct rainfall modelling' (also referred to as 'rain-on-grid') scheme. The hydraulic model also considers the existence of two culverts located in the area. The model has been built on a fine-scale (0.2 m) resolution digital terrain model representing the major buildings in the region including the monument itself.

Results suggest that the flood hazard is not significant in the region of direct proximity to the monument (Tower of the Winds), but other flood-prone areas in the Agora (such as the lower terrain region where the Peristyle is located) have been identified. In this case, the flood risk is mainly related to issues regarding the accessibility of visitors to the archaeological site after a major storm event and the requirement to clean the site and its exhibits due to stagnant water. Visualization of these results is made possible through the ARCHYTAS platform which allows the user to design a synthetic scenario based on the selection of a specific event duration, return period, and soil infiltration capacity (e.g., based on the user's assessment of the antecedent soil moisture content, i.e., wet, average, or dry conditions) and assess the resulting flood map. This is made possible using a database of readily available scenarios and corresponding flood maps, thus minimizing the computational burden which is otherwise critical in this type of hydraulic model [34,35]. An update of the system may also allow the development of an early flood warning system for actual rainfall events, by coupling the platform with a local rain gauge and retrieving flood maps based on similarity criteria.

An important limitation of the analysis is the lack of 'hard' validation data, as only the locals' experiences are available for the study area. Unfortunately, this is a common limitation of most studies in urban areas, in which 'soft' data are usually the norm and are only made available after catastrophic events [36]. This is the reason why various scenarios are run to reflect a range of uncertainty in the maximum flood depth maps. In addition, it is argued that, in view of the large uncertainty involved in urban flood mapping, the 'direct rainfall modelling' scheme applied over a very detailed digital terrain model introduces some physical basis in the routing of the stormwaters that bypasses several limitations of the conventional methodology of hydrograph routing. The latter typically requires more assumptions including the separate rainfall-runoff modelling that must be performed prior to the hydrograph routing process which is itself not applicable in the absence of surface streams. Due to these advantages, we consider the direct rainfall scheme to be a promising direction for the reliable estimation of flood risk in sites of cultural heritage and other vulnerable urban areas where detailed assessments may be required and high-quality topographic data can be made available.

Author Contributions: Conceptualization, T.I., P.D. and D.K.; methodology, T.I., P.D. and D.K.; software, T.I. and P.D.; validation, T.I., P.D. and D.K.; formal analysis, T.I.; investigation, T.I.; resources, T.I.; data curation, T.I.; writing—original draft preparation, T.I.; writing—review and editing, P.D. and D.K.; visualization, T.I.; supervision. D.K.; project administration, D.K.; funding acquisition, D.K. All authors have read and agreed to the published version of the manuscript.

Funding: This research was funded by the European Regional Development Fund of the European Union and Greek national funds through the Operational Program of Competitiveness, Entrepreneurship and Innovation, under the call RESEARCH—CREATE—INNOVATE (project code: T1EDK-00956), project «ARCHYTAS: archetypal telemetry and decision support system for the protection of monumental structures».

Data Availability Statement: The data presented in this study are available on request from the corresponding author.

Acknowledgments: We greatly thank Vlasis Koumousis and Dimitrios Vamvatsikos for the coordination and administration of the ARCHYTAS project and Alexandros Manetas for integrating the results into the ARCHYTAS platform. We are grateful to the anonymous reviewers for their helpful comments.

Conflicts of Interest: The authors declare no conflict of interest.

References

1. Camuffo, D.; Del Monte, M.; Ongaro, A. The pH of the atmospheric precipitation in Venice, related to both the dynamics of precipitation events and the weathering of monuments. *Sci. Total Environ.* **1984**, *40*, 125–139. [CrossRef]
2. Arnold, A.; Zehnder, K. Salt weathering on monuments. In *The Conservation of Monuments in the Mediterranean Basin: The Influence of Coastal Environment and Salt Spray on Limestone and Marble, Proceedings of the 1st International Symposium, Bari, Italy, 7–10 June 1989*; La Conservazione Dei Monumenti Nel Bacino Mediterraneo: Influenza Dell Ambiente Costiero e Dello Spray Marino Sulla Pietra Calcareo e Sul Marmo; Atti Del 1 Simposio Internazionale: Bari, Italy, 1990; pp. 31–58.
3. Ortega-Calvo, J.J.; Ariño, X.; Hernandez-Marine, M.; Saiz-Jimenez, C. Factors affecting the weathering and colonization of monuments by phototrophic microorganisms. *Sci. Total Environ.* **1995**, *167*, 329–341. [CrossRef]
4. Al-Weshah, R.; El-Khoury, F. Flood risk mitigation using watershed management tools: Petra area (Jordan). In *Risk-Based Decision Making in Water Resources IX*; ASCE: Reston, VA, USA, 2001; pp. 164–172.
5. Fitzner, B.; Heinrichs, K.; La Bouchardiere, D. Weathering damage on Pharaonic sandstone monuments in Luxor-Egypt. *Build. Environ.* **2003**, *38*, 1089–1103. [CrossRef]
6. Lanza, S.G. Flood hazard threat on cultural heritage in the town of Genoa (Italy). *J. Cult. Herit.* **2003**, *4*, 159–167. [CrossRef]
7. Heinrichs, K. Diagnosis of weathering damage on rock-cut monuments in Petra, Jordan. *Environ. Geol.* **2008**, *56*, 643–675. [CrossRef]
8. Camuffo, D. *Microclimate for Cultural Heritage: Measurement, Risk Assessment, Conservation, Restoration, and Maintenance of Indoor and Outdoor Monuments*; Elsevier: Amsterdam, The Netherlands, 2019.
9. Hatır, M.E. Determining the weathering classification of stone cultural heritage via the analytic hierarchy process and fuzzy inference system. *J. Cult. Herit.* **2020**, *44*, 120–134. [CrossRef]
10. Reiche, P. Graphic representation of chemical weathering. *J. Sediment. Res.* **1943**, *13*, 58–68.
11. Camuffo, D. Physical weathering of stones. *Sci. Total Environ.* **1995**, *167*, 1–14. [CrossRef]
12. Wang, J.-J. Flood risk maps to cultural heritage: Measures and process. *J. Cult. Herit.* **2015**, *16*, 210–220. [CrossRef]
13. Gandini, A.; Egusquiza, A.; Garmendia, L.; San-José, J.-T. Vulnerability assessment of cultural heritage sites towards flooding events. In *IOP Conference Series: Materials Science and Engineering*; IOP Publishing: Bristol, UK, 2018; p. 012028.
14. Galloway, G.E.; Seminara, G.; Blöschl, G.; García, M.H.; Montanari, A.; Solari, L. Reducing the Flood Risk of Art Cities: The Case of Florence. *J. Hydraul. Eng.* **2020**, *146*, 02520001. [CrossRef]
15. Dimitriadis, P.; Tegos, A.; Oikonomou, A.; Pagana, V.; Koukouvinos, A.; Mamassis, N.; Koutsoyiannis, D.; Efstratiadis, A. Comparative evaluation of 1D and quasi-2D hydraulic models based on benchmark and real-world applications for uncertainty assessment in flood mapping. *J. Hydrol.* **2016**, *534*, 478–492. [CrossRef]
16. Mignot, E.; Paquier, A.; Haider, S. Modeling floods in dense urban areas using 2D shallow water equations. *J. Hydrol.* **2006**, *327*, 186–199. [CrossRef]
17. Yu, D.; Lane, S.N. Urban fluvial flood modelling using a two-dimensional diffusion-wave treatment, part 1: Mesh resolution effects. *Hydrol. Process. Int. J.* **2006**, *20*, 1541–1565. [CrossRef]
18. Bellos, V.; Kourtis, I.M.; Moreno-Rodenas, A.; Tsihrintzis, V.A. Quantifying roughness coefficient uncertainty in urban flooding simulations through a simplified methodology. *Water* **2017**, *9*, 944. [CrossRef]
19. Soares-Frazão, S.; Lhomme, J.; Guinot, V.; Zech, Y. Two-dimensional shallow-water model with porosity for urban flood modelling. *J. Hydraul. Res.* **2008**, *46*, 45–64. [CrossRef]
20. David, A.; Schmalz, B. A Systematic Analysis of the Interaction between Rain-on-Grid-Simulations and Spatial Resolution in 2D Hydrodynamic Modeling. *Water* **2021**, *13*, 2346. [CrossRef]
21. Vamvatsikos, D.; Fragiadakis, M.; Georgopoulos, I.O.; Koumousis, V.K.; Koutsoyiannis, D.; Manetas, A.; Melissianos, V.E.; Papadopoulos, C.; Papanikolopoulos, K.E.; Toumpakari, E.E. The ARCHYTAS Intelligent Decision-Support System for the Protection of Monumental Structures. In *Protection of Historical Constructions: Proceedings of the PROHITECH, Athens, Greece, 25–27 October 2021*; Springer International Publishing: Berlin/Heidelberg, Germany, 2022; Volume 4, pp. 1246–1255.
22. *Ministry of Culture, Archaeological Bulletin*; Publishing: Hellenic Organization of Cultural Resources Development: Athens, Greece, 2000; Volume 55.
23. *Ministry of Culture, Archaeological Bulletin*; Publishing: Hellenic Organization of Cultural Resources Development: Athens, Greece, 1985; Volume 40.
24. Iliopoulou, T.; Koutsoyiannis, D. A parsimonious approach for regional design rainfall estimation: The case study of Athens. In Proceedings of the 7th IAHR Europe Congress, Athens, Greece, 7–9 September 2022.
25. Koutsoyiannis, D.; Xanthopoulos, T. *Technical Hydrology*, 3rd ed.; National Technical University: Athens, Greece, 1999; 418p.
26. Koutsoyiannis, D. A stochastic disaggregation method for design storm and flood synthesis. *J. Hydrol.* **1994**, *156*, 193–225. [CrossRef]
27. Sutcliffe, J.V. *Methods of Flood Estimation, A Guide to Flood Studies Report*; Report No 49; Institute of Hydrology: Wallingford, UK, 1978.
28. Chow, V.T.; Maidment, D.R.; Mays, L.W. *Applied Hydrology*; McGraw-Hill: New York, NY, USA, 1988; 572p.
29. US Soil Conservation Service. *National Engineering Handbook*; Section 4; Hydrology, U.S. Department of Agriculture, U.S. Government Printing Office: Washington, DC, USA, 1972.

30. United States Department of Agriculture. Urban Hydrology for Small Watersheds (PDF). Technical Release 55 (TR-55) (Second ed.). Natural Resources Conservation Service, Conservation Engineering Division. 1986. Available online: https://www.nrc.gov/docs/ML1421/ML14219A437.pdf (accessed on 19 November 2023).
31. Hydrologic Engineering Center. *HEC-RAS 2D Modeling User's Manual*; U.S. Army Corps of Engineers: Davis, CA, USA, 2021.
32. Courant, R.; Friedrichs, K.; Lewy, H. On the partial difference equations of mathematical physics. *IBM J. Res. Dev.* **1967**, *11*, 215–234, (republication in *Math. Ann.* **1928**, *100*, 32–74). [CrossRef]
33. Chow, V.T. *Open Channel Hydraulics*; McGraw-Hill: New York, NY, USA, 1959.
34. Henonin, J.; Russo, B.; Mark, O.; Gourbesville, P. Real-time urban flood forecasting and modelling–a state of the art. *J. Hydroinformatics* **2013**, *15*, 717–736. [CrossRef]
35. Teng, J.; Jakeman, A.J.; Vaze, J.; Croke, B.F.; Dutta, D.; Kim, S. Flood inundation modelling: A review of methods, recent advances and uncertainty analysis. *Environ. Model. Softw.* **2017**, *90*, 201–216. [CrossRef]
36. Tegos, A.; Ziogas, A.; Bellos, V.; Tzimas, A. Forensic hydrology: A complete reconstruction of an extreme flood event in data-scarce area. *Hydrology* **2022**, *9*, 93. [CrossRef]